Chinese Chemical Letters 37 (2026) 111758

Contents lists available at ScienceDirect

Chinese Chemical Letters

journal homepage: www.elsevier.com/locate/cclet

Therapeutic improvement of adenomyosis by supramolecular cells-based macrophage membrane-encapsulated dydrogesterone nanoparticles *via* targeted drug delivery and inhibition of inflammation in the uterus

Renwen Zhang, Yixing Zou, Aihua Liao*, Jing Luo*

Institute of Reproductive Health, Center for Reproductive Medicine, Tongji Medical College, Huazhong University of Science and Technology, Wuhan 430030, China

ARTICLE INFO

Article history:
Received 27 May 2025
Revised 25 August 2025
Accepted 27 August 2025
Available online 28 August 2025

Keywords:
Adenomyosis
Supramolecular cells
Macrophage membrane
Epithelial-mesenchymal transition
Anti-inflammatory
Therapeutic efficacy

ABSTRACT

Adenomyosis remains a poorly understood condition characterized by the limited efficacy of current pharmacotherapy. Traditional treatments using dydrogesterone (DG) for adenomyosis often yield suboptimal outcomes due to poor targeting and susceptibility to immune rejection. Therefore, there is an urgent need to identify an effective approach to enhancing the therapeutic efficacy of DG. Given the enrichment of macrophages in the uterus associated with adenomyosis, this study sought to develop a supramolecular cell-based macrophage membrane-encapsulated DG nanoparticle (MM-DG-NP) delivery system for targeted drug delivery and effective treatment of adenomyosis. The MM-DG-NP system leverages a multifaceted therapeutic mechanism by evading phagocytic clearance and enhancing targeted drug delivery efficacy. The supramolecular cell framework, constructed through dynamic non-covalent interactions, provides structural stability and biofunctional adaptability to the MM-DG-NP system, enabling precise homing to uterine macrophage-rich pathological sites. The MM-DG-NP system demonstrated therapeutic efficacy superior to that of traditional DG therapy in murine models, characterized by a pronounced reduction in endometrial invasion depth within the myometrium; effective inhibition of epithelial–mesenchymal transition (EMT) progression in the glandular epithelium; significant attenuation of local inflammatory cytokine release in the uterus, including interleukin-6 (IL-6), tumor necrosis factor-alpha (TNF-α), and interferon-gamma (IFN-γ); and notable alleviation of pain responses. These results highlight the critical role of supramolecular cell engineering in enhancing the biocompatibility and targeting precision of nanomedicines. MM-DG-NPs thus represent a promising strategy for overcoming current pharmacotherapeutic limitations in adenomyosis, warranting further investigation to explore their potential clinical translation.

© 2026 Published by Elsevier B.V. on behalf of Chinese Chemical Society and Institute of Materia Medica, Chinese Academy of Medical Sciences.

Adenomyosis, a complex gynecological disorder characterized by ectopic endometrial tissue invasion into the myometrium, imposes a substantial clinical burden on 20%–35% of reproductive-aged women, with peak incidence occurring between 40 and 49 years [1–4]. Despite its high prevalence and debilitating symptoms, no pharmacological agent has been specifically approved for the treatment of adenomyosis. Current therapeutic strategies rely predominantly on pharmacological interventions (*e.g.*, progestins) and surgical approaches, although no dedicated therapeutic agents have been approved specifically for adenomyosis in clinical practice, necessitating off-label use of endometriosis-targeted medications or symptomatic management [5–8]. Against this backdrop, progestogens such as dydrogesterone (DG) have emerged as first-line pharmacological options because of their cost-effectiveness, favorable tolerability profile, and clinical advantages, including ovulation preservation, lack of androgen receptor interaction, and convenience of administration. These attributes align particularly well with the needs of patients prioritizing natural reproduction [6,9]. However, despite their established role in short-term management, long-term progestogen-based regimens face escalating challenges, notably acquired drug resistance and insufficient lesion-targeting precision [6,9]. Surgical interventions, although definitive, often compromise fertility [5], underscoring the urgent need for innovative drug delivery systems capable of overcoming biological bar-

* Corresponding authors.
E-mail addresses: aihua_liao@hust.edu.cn (A. Liao), luojing117@hust.edu.cn (J. Luo).

https://doi.org/10.1016/j.cclet.2025.111758
1001-8417/© 2026 Published by Elsevier B.V. on behalf of Chinese Chemical Society and Institute of Materia Medica, Chinese Academy of Medical Sciences.

riers while preserving reproductive function. Based on the aforementioned clinical challenges and unmet therapeutic needs, this study sought to develop an innovative drug delivery system that addresses both the limitations of conventional progestogen therapies and the biological barriers inherent in adenomyosis treatment.

Emerging insights into the pathophysiology of adenomyosis reveal a hormone–immunity crosstalk mechanism [10–12]. Chronic hyperestrogenism induces oxytocin-mediated uterine mechanical stress, triggering focal inflammation characterized by macrophage polarization [13,14]. Anti-inflammatory cytokines (*e.g.*, transforming growth factor-beta 1 (TGF-β1) and interleukin-10 (IL-10)) and pro-inflammatory cytokines (*e.g.*, IL-1 and tumor necrosis factor-alpha (TNF-α)) drive epithelial–mesenchymal transition (EMT) and sustain lesion progression [15–17]. Notably, macrophage infiltration within adenomyotic tissue correlates positively with disease severity [18–21], underscoring their central role as both mediators of disease pathology and potential therapeutic targets.

Building on these mechanistic insights, recent advances in biomimetic nanotechnology offer a promising avenue for targeted therapeutic intervention. Recent advances in biomimetic nanotechnology offer novel therapeutic potential for reproductive disease intervention. Despite enhancing drug solubility and half-life, conventional nano-drug delivery systems (NDDS) face rapid clearance by the mononuclear phagocyte system (MPS) [22–24]. In contrast, biomimetic cell membrane encapsulation technology enables high-fidelity transfer of source cell membrane proteins onto synthetic nanoparticle cores *via* extrusion or sonication, thereby effectively circumventing phagocytic elimination by monocytes and prolonging systemic circulation [25–27]. This immunoevasive property, combined with intrinsic homing capabilities conferred by membrane-derived adhesion molecules, positions biomimetic NDDS as a transformative platform for targeted therapeutic delivery in tumors and inflammatory diseases. Nevertheless, the application of such platforms in to adenomyosis remains unexplored. Given the important role of macrophages in the pathogenesis of adenomyosis, we hypothesized that macrophage membrane (MM)-coated nanoparticles could act as both lesion-targeted drug carriers and immune-modulatory agents for effective adenomyosis therapy.

This study established a MM-coated DG nanoparticle (MM-DG-NP) platform for adenomyosis therapy, validated through comprehensive physicochemical and biological characterization. Particle size, zeta potential, and morphological features were assessed using dynamic light scattering (DLS) and transmission electron microscopy (TEM), confirming the successful fabrication of structurally uniform, membrane-coated nanoparticles (Fig. 1). To validate the feasibility and biological relevance of this platform, we conducted integrated *in vitro* and *in vivo* studies. *In vitro* experiments demonstrated enhanced immune evasion (*e.g.*, reduced phagocytosis), while *in vivo* assessments in a hormone-induced murine model confirmed lesion-specific nanoparticle accumulation and therapeutic efficacy. Furthermore, based on the pivotal role of EMT and chronic inflammation in disease progression, we elucidated MM-DG-NPs' dual regulatory effects on EMT suppression and inflammatory cytokine attenuation. Furthermore, based on the pivotal role of EMT and chronic inflammation in disease progression, we elucidated MM-DG-NPs' dual regulatory effects on EMT suppression and inflammatory cytokine attenuation.

MM-DG-NPs were synthesized through a three steps process: (i) Formulation of DG nanoparticles (DG-NPs), DG-NPs are prepared by first dissolving the hydrophobic drug in dimethyl sulfoxide (DMSO), followed by slow dropwise addition of the resulting solution into an aqueous medium. As DMSO disperses in water, the drug, with negligible solubility in the polar aqueous environment, precipitates and undergoes physical aggregation, driven by hydrophobic interactions that minimize contact with water molecules. (ii) Isolation of MMs from murine RAW264.7 cells, and

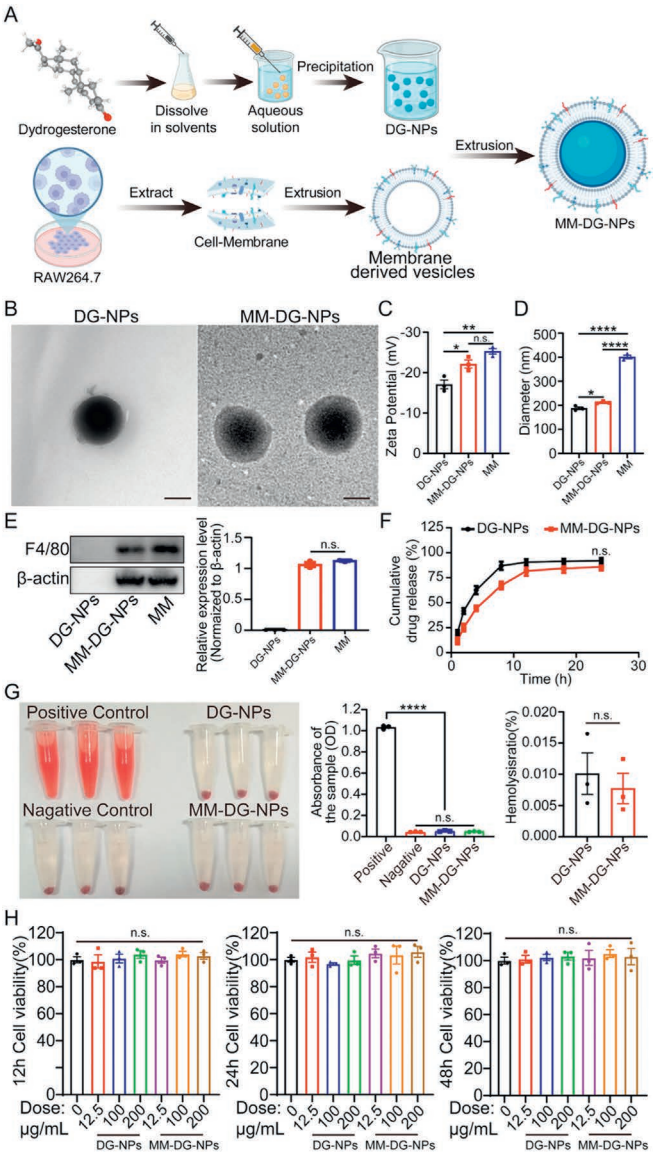


Fig. 1. Characterization and safety assessment of DG-NPs and MM-DG-NPs. (A) Illustration of preparation process for DG-NPs and MM-DG-NPs. (B) TEM images of DG-NPs and MM-DG-NPs. Scale bar: 100 nm. (C) Zeta potentials of DG-NPs, DG-MM-NP, and MM analyzed by DLS. (D) Particle sizes of NPs and MM-NPs analyzed by DLS. (E) Representative Western blots of F4/80 in DG-NPs, DG-MM-NP and MM. (F) *In vitro* drug release profiles of DG-NPs and MM-DG-NPs. (G) Images of hemolysis tests conducted on DG-NPs and MM-DG-NPs following centrifugation and their respective absorbance and hemolysis rates. (H) Cell proliferation of mouse endometrial cells treated with different concentrations (0, 12.5, 100 and 200 μg/mL) of DG-NPs and MM-DG-NPs was detected by CCK-8 assays. Data are presented as mean ± standard error of the mean (SEM) ($n = 3$). $^{*}P < 0.05$, $^{**}P < 0.01$, $^{****}P < 0.0001$. n.s., not significant.

(iii) membrane cloaking of DG-NPs *via* extrusion (Fig. 1A). Transmission electronic microscope (TEM) images confirmed that the resulting MM-DG-NPs were spherical particles with nanometer-scale dimensions and high monodispersity (Fig. 1B). DLS analysis showed a more negative zeta potential for MM-DG-NPs compared to uncoated DG-NPs (Figs. 1C and D), and the hydrodynamic diameter of the MM-DG-NPs was 211.88 nm. Immunoblotting confirmed the presence and enrichment of critical surface antigens, including F4/80, on MM-DG-NPs, indicating successful translocation of the MM onto the nanoparticles (Fig. 1E). Drug release studies conducted in buffer solutions simulating the extracellular environment (phosphate buffered saline, pH 7.4) demonstrated sus-

tained release progiles for both DG-NPs and MM-DG-NPs, with 90.46 % and 81.60 % of the encapsulated drug released after 12 h, respectively. Compared to DG-NPs, MM-DG-NPs exhibited a slightly slower DG release profile (Fig. 1F). These physicochemical characteristics, combined with the engineered biomimetic surface, form the foundation for subsequent biological evaluation of the nanocarriers. The slightly slower release observed in MM-DG-NPs suggests that membrane encapsulation imparts additional diffusion resistance, which may support extended systemic circulation (Fig. 1F). At 24 h post-initiation, the release percentages reached 91.80 % and 85.63 % for DG-NPs and MM-DG-NPs respectively, with no statistically significant difference between the two groups. Collectively, these physicochemical properties, combined with the biomimetic surface engineering, establish the MM-DG-NP platform as a viable candidate for sustained and targeted drug delivery. To ensure consistency and reproducibility throughout the production process, a comprehensive set of quality control specifications was established to monitor key physicochemical and biological properties of MM-DG-NPs. These specifications were designed to maintain the consistency and reliability of the nanoparticles, thereby enhancing their safety and effectiveness for intended applications.

The *in vitro* and *in vivo* biological effects of the nanoparticle formulations were systematically evaluated, starting with the assessment of blood compatibility, a critical parameter for biomaterials intended for systemic administration. Hemolysis tests were conducted by exposing DG-NPs and MM-DG-NPs directly to whole blood at concentrations up to 200 μg/mL. The resulting optical density (OD) measurements revealed no significant increase in hemolysis relative to the negative control, indicating minimal red blood cell lysis, further corroborating their non-hemolytic properties (Fig. 1G).

Having established the basic safety profile, we further assessed the biocompatibility of these nanocarriers in cellular and whole-organism contexts. The biocompatibility of the DG-NPs and MM-DG-NPs at the cellular level was evaluated using cell counting kit-8 (CCK-8) cell proliferation assay. Cells were exposed to increasing concentrations of nanoparticles for 12, 24, and 48 h of incubation. Both nanoparticle formulations demonstrated high biocompatibility, with no significant cytotoxicity observed at any time point or up to a concentration of 200 μg/mL (Fig. 1H), indicating their stability *in vitro*.

To comprehensively assess long-term safety, hematological analysis, biochemical parameters, and histological analyses of major organs were performed 21 days after the systemic administration of the nanocarriers. As shown in Fig. S1 (Supporting information), no statistically significant differences were observed in hematological profiles or biochemical markers across treatment groups (Figs. S1A and B), and no discernible morphological abnormalities were observed in the heart, liver, spleen, lungs, or kidneys across the treatment groups (Fig. S1C). These results further corroborate the favorable biocompatibility of both nanparticle formulations, supporting their suitability for extended *in vivo* applications.

With the safety profile established, we next developed and vadilated a preclinical murine model of adenomyosis for therapeutic evaluation. All animal procedures in this study were approved by Ethical Approval Formal Review of Experimental Animal Ethics, Huazhong University of Science and Technology ([2022] IACUC Number: 3916). It followed all guidelines, regulations, legal, and ethical standards as required for animals and was approved under the National Guidelines for Animal Protection. As shown in Fig. S2 (Supporting information), a mouse model of adenomyosis was established using a tamoxifen-induced protocol, as previously described (Fig. S2A) [28,29]. Histological examination of uterine tissue was conducted at 12 weeks to confirm the presence of adenomyosis following tamoxifen administration. In the control group, the myometrium exhibited a tissue structure characterized by a uniformly concentric arrangement. In contrast, tissue alterations in the intervention group were markedly disorganized, with glands dispersed throughout the uterine wall (Fig. S2B). Mori classification revealed a significant difference between the control and intervention groups, with the intervention group exhibiting a superior classification grade for adenomyosis (Figs. S2C and D) [30]. As previous studies have found, a substantial difference was evident in the tail-flick test results between the control and intervention mice at 12 weeks (Figs. S2E and F). The mice in the intervention group displayed a significant increase in thermal tolerance. The results of the present study demonstrated a high prevalence of adenomyosis in the intervention group at 12 weeks, and the findings were highly reproducible, paving the way for subsequent modeling and treatment studies. Importantly, this model reliably reproduced the hallmark pathological features of human adenomyosis, including elevated immune infiltration patterns in affected tissue (Fig. S2G), which supports its use in subsequent studies.

Armed with a validated disease model, we then systematically evaluated the therapeutic efficacy of MM-DG-NPs in a three-week treatment regimen. To assess the therapeutic efficacy following three weeks of uninterrupted treatment in various treatment groups, we conducted a histological analysis of the mouse uteri (Figs. 2A–C). Compared with the untreated, DG groups, the administration of DG-NPs and MM-DG-NPs significantly reduced endometrial gland invasion into the myometrium. In addition, the integrity of the myometrium was partially restored. These findings indicate that DG-NPs and MM-DG-NPs exhibited superior therapeutic effects over a three-week treatment period. Mori's classification based on uterine morphology demonstrated a decrease in the severity of adenomyosis in mice following treatment with DG, DG-NPs, and MM-DG-NP (Fig. 2D). The results of the tail-flick test indicated a partial improvement in the pain of the mice (Fig. 2E). The improved therapeutic efficacy stemmed from the nanocarriers' dual capability to evade immune clearance and selectively accumulate at lesion sites. Demonstrated reduction in phagocytic uptake (Fig. 2F) confirmed effective MM integration, while corresponding immunological profiling revealed enhanced targeting precision of membrane-encapsulated DG-NPs in adenomyosis treatment (Fig. 2G).

Adenomyosis is a highly aggressive disease affecting the endometrium [4]. EMT has a significant influence on the development of this transition. Consequently, we conducted a comprehensive study using both *in vivo* and *in vitro* experiments to investigate the effects of DG-NPs and MM-DG-NPs on EMT.

First, we performed an immunohistochemical analysis of the mouse uterus in each treatment group. Our findings revealed that EMT-related proteins were expressed during the progression of uterine adenomyosis, corroborating the results of previous studies [31–36]. EMT in the uterus of mice treated with DG-NPs and MM-DG-NPs was partially suppressed (Fig. 3A and Fig. S3A in Supporting information). Second, primary mouse endometrial cells were used for *in vitro* experiments. The results demonstrated significant inhibition of the migratory ability of endometrial cells upon treated with DG-NPs and MM-DG-NPs (Fig. 3B). Besides, cells were examined to assess the presence of proteins associated with EMT. The results revealed an increase in the expression of E-cadherin and a decrease in the expression of vimentin, β-catenin, lymphoid enhancer-binding factor 1 (LEF1), wingless-type MMTV integration site family member 5a (WNT5a) after treated with DG-NPs and MM-DG-NPs (Figs. 3C and D, Fig. S3 in Supporting information). These findings indicate that DG-NPs and MM-DG-NPs exert their therapeutic effects by regulating the epithelial-mesenchymal transition (EMT) process. To further validate these findings in a human-relevant context, we extended our investigation to Ishikawa cells, a widely utilized human endometrial cell line. Functional assays

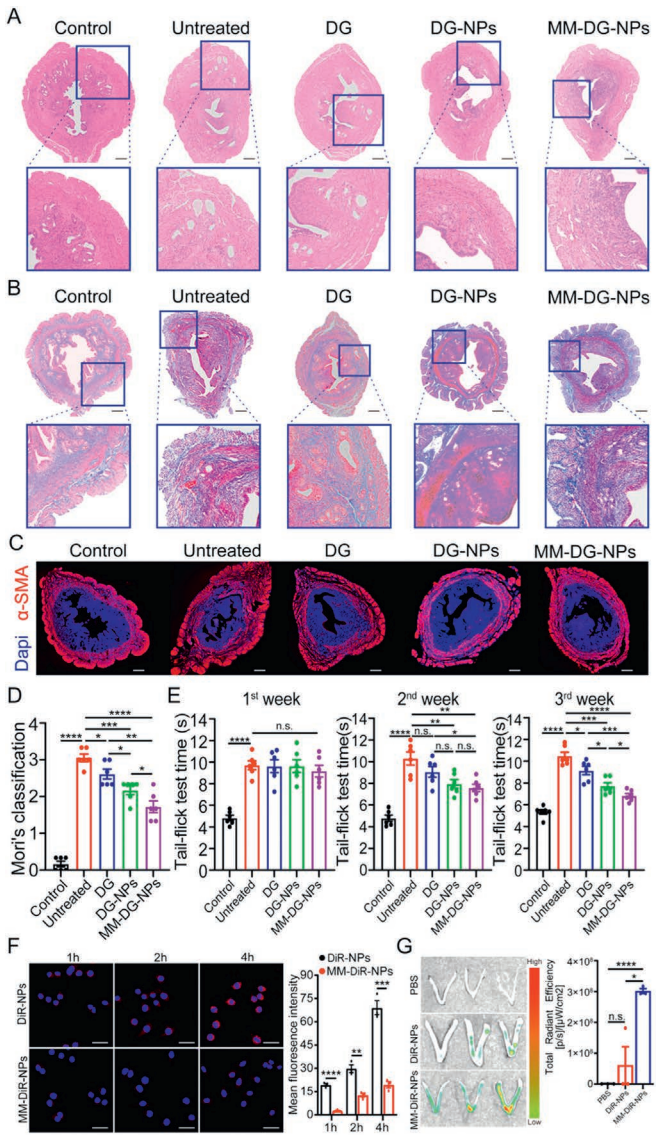


Fig. 2. Evaluation of DG-NPs and MM-DG-NPs treatment effects. (A) Histological analysis of mouse uteri from different treatment groups. (B) Masson stain of mouse uteri from different treatment groups. (C) Immunofluorescence analysis of alpha-smooth muscle actin (α-SMA) (red) and 4′,6-diamidino-2-phenylindole (DAPI) (blue) in mouse uteri from different treatment groups. Scale bar: 200 μm. (D) Mori's classification of mouse uteri from different treatment groups ($n = 6$). (E) Tail-flick test from different treatment groups ($n = 6$). (F) Immune escape assay of DG-NPs and MM-DG-NPs against RAW264.7 ($n = 3$). Scale bar: 20 μm. (G) Quantitative analysis of DiR-labeled NPs-DG and MM-NPs-DG in utero fluorescent signals 4 h after injection ($n = 3$). Data are presented as mean ± SEM. $^{*}P < 0.05$, $^{**}P < 0.01$, $^{***}P < 0.001$, $^{****}P < 0.0001$.

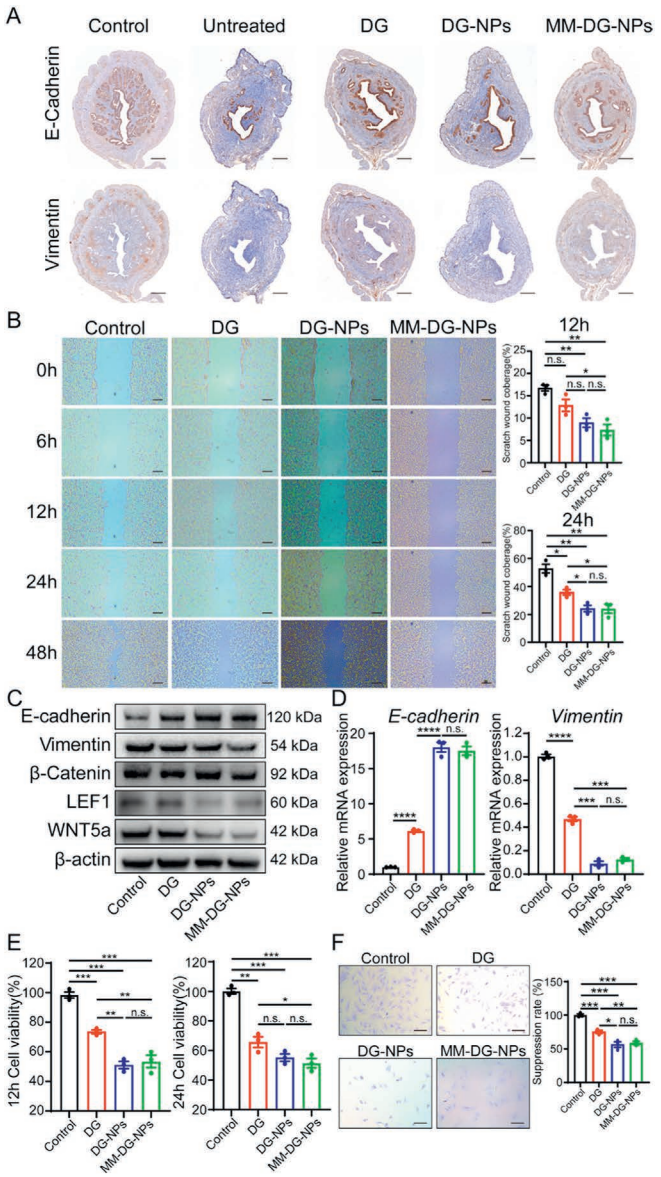


Fig. 3. DG-NPs and MM-DG-NPs treats adenomyosis by inhibiting EMT. (A) Immunohistochemistry of mouse uterus in different treatment groups. Scale bar: 200 μm. (B) Effect of different intervention groups on migratory capacity of mouse endometrial cells. Scale bar: 250 μm. (C) Representative Western blots of EMT-associated proteins E-cadherin, vimentin, β-catenin, LEF1 and WNT5a in mouse uterine endometrial cells in different intervention groups. (D) mRNA expression of E-cadherin and vimentin in mouse uterine endometrial cells under effect of different intervention groups. (E) Effect of different intervention groups on Ishikawa cell viability detected by CCK-8 assay. (F) Effect of different intervention groups on proliferative capacity of Ishikawa cells. Scale bar: 20 μm. Data are presented as mean ± SEM ($n = 3$). $^{*}P < 0.05$, $^{**}P < 0.01$, $^{***}P < 0.001$, $^{****}P < 0.0001$.

combined with protein and mRNA analyses of these cells revealed that the treatment with DG-NPs and MM-DG-NPs significantly inhibited cell proliferation and migration, as well as downregulated protein expression in the TGF-β/Smad signaling pathway implicated in EMT processes (Figs. 3E and F; Figs. S3B, C and S4 in Supporting information). These findings provide valuable insights into potential clinical applications of this nanoparticle drug.

In addition to regulating EMT, we examined the effects of DG-NPs and MM-DG-NPs on the inflammatory microenvironment, a hallmark of adenomyosis progression. A multi-platform analysis using immunohistocytochemistry (IHC), enzyme-linked immunosorbent assay (ELISA), and flow cytometry revealed significant suppression of uterine pro-inflammatory cytokines across treatment groups (Figs. 4A–C). These results were supported by *in vitro* assays, which showed dose-dependent inhibition of inflammatory mRNA expression in endometrial cells (Fig. 4D). Together, these findings confirmed that MM-DG-NPs simultaneously modulate EMT and inflammatory signaling pathways, establishing a dual mechanism of therapeutic action.

Notably, while exhibiting comparable therapeutic effects overall, MM-DG-NPs showed superior *in vivo* efficacy despite equivalent *in vitro* performance. Mechanistically, phagocytosis assays with RAW264.7 cells demonstrated a significantly reduced uptake of MM-DG-NPs compared to DG-NPs over time (Fig. 2F), which is attributable to MM encapsulation conferring enhanced immune-evasive properties that potentiate *in vivo* therapeutic advantages.

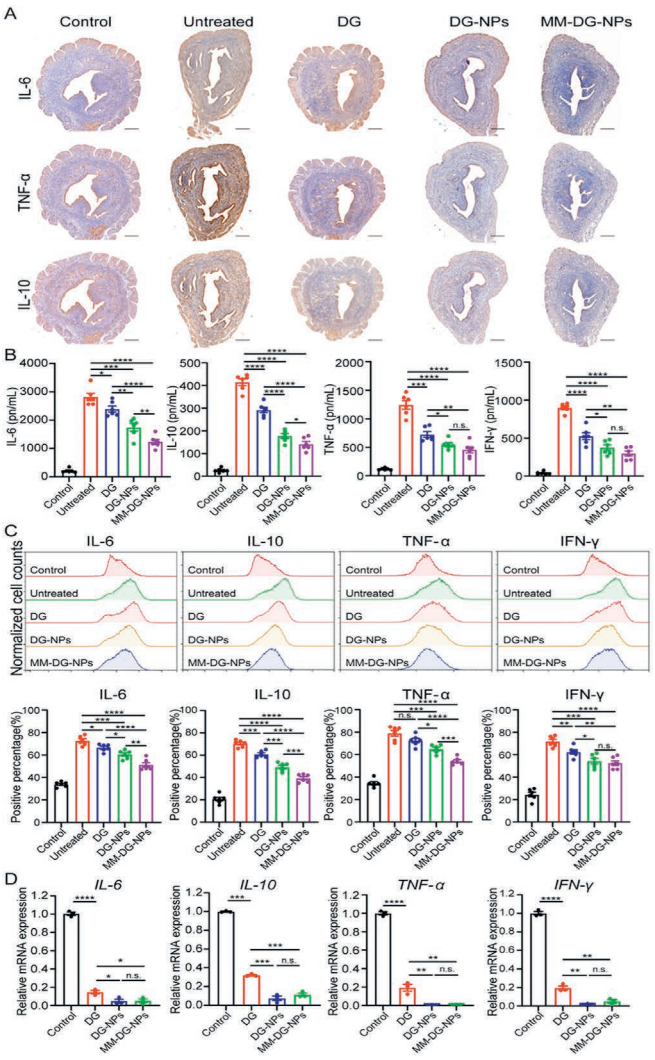


Fig. 4. DG-NPs and MM-DG-NPs treat adenomyosis by suppressing inflammation. (A) Immunohistochemistry of IL-6, TNF-α, IL-10 in mouse uterus under effect of different intervention groups. Scale bar: 200 μm. (B) ELISA for inflammatory factors in mouse uterine under influence of different intervention groups ($n = 6$). (C) Flow cytometry detection of inflammatory factor expression in mouse uterine leucocytes ($n = 6$). (D) Inflammatory factor mRNA expression in mouse uterine endometrial cells under effect of different intervention groups ($n = 3$). Data are presented as mean ± SEM. $^{*}P < 0.05$, $^{**}P < 0.01$, $^{***}P < 0.001$, $^{****}P < 0.0001$.

Adenomyosis remains a presistent therapeutic challenge that is compounded by the lack of disease-specific pharmacotherapies and the reliance on off-label use of endometriosis drugs without dosage or formulation optimization [8]. Although non-steroidal anti-inflammatory drugs and steroids remain first-line options, their transient efficacy and systemic toxicity underscore the critical need for targeted delivery systems that balance therapeutic potency with minimized off-target effects. In response to these limitations, we developed a MM-biomimetic nanoparticle platform designed to address these dual challenges through biologically inspired engineering, capitalizing on DG's dual advantage in fertility preservation and inflammation modulation as a progesterone receptor modulator.

Conventional nanomedicine strategies, although promising in enhancing drug solubility and passive accumulation *via* enhanced permeability and retention [37–39], face inherent limitations in adenomyosis due to rapid clearance by the MPS and poor inflammatory tropism. By encapsulating nanoparticles of DG within MMs, our biomimetic system leverages the innate biological functions of macrophages to overcome these barriers. The MMs coating not only shields nanoparticles from MPS recognition but also directs active homing to adenomyosis lesions through chemokine receptor-mediated trafficking, mirroring the recruitment of native macrophages to inflammatory sites [40,41].

Beyond drug delivery, the reduction of EMT and inflammation in the adenomyosis environment may explain the attenuation effects of MM-DG-NPs. A key pathogenic mechanism underlying adenomyosis involves the disruption and subsequent repair of the affected tissue [13]. This process is accompanied by EMT induction, inflammatory cell infiltration, and the increased release of both pro-inflammatory (*e.g.*, IL-6 and TGF-β) and anti-inflammatory (*e.g.*, IL-10) cytokines, resulting in the disruption of the inflammatory microenvironment and epithelial cell migration across the myometrium. Under the pharmacological action of DG, these cytokines are suppressed within lesions, reducing their local concentrations and disrupting the feedforward loop of inflammation and EMT. This multimodal action, simultaneously inhibiting EMT markers (α-SMA and vimentin) while restoring epithelial integrity (E-cadherin), led to a reduction in adenomyosis lesion area in murine models, outperforming both DG alone and non-targeted DG-NPs. Notably, while macrophage-inspired platforms have demonstrated efficacy in the treatment of atherosclerosis [42] and rheumatoid arthritis [43], this study pioneers their application in gynecopathology, capitalizing on shared inflammatory pathways while circumventing challenges unique to targeting reproductive tissue.

A critical distinction lies in our platform's safety profile compared to that of live macrophage-based carriers. Although prior studies utilizing internalized nanoparticle-laden macrophages reported higher lesion accumulation [44], their propensity for inflammatory activation within the disease microenvironment may paradoxically exacerbate pathology. In contrast, acellular MM coatings retain targeting functionality without cellular reactivity. This advantage aligns with MM-based strategies for treating atherosclerosis [42] and rheumatoid arthritis [43], reflecting the expanding frontier of cell membrane-engineered nanotherapeutics in spatially complex inflammatory disorders.

The translational implications of this technology extend beyond adenomyosis. The modular design permits adaptation to diverse stimuli (*e.g.*, pH and enzymatic activity) for context-specific drug release [45,46]. At the same time, interchangeable membrane sources, such as patient-derived macrophages or engineered cell lines, could enhance the personalization of targeting specificity [47–52]. Furthermore, co-encapsulation with complementary agents (*e.g.*, anti-angiogenic compounds) may synergistically address multifactorial aspects of adenomyosis progression, including neovascularization and fibrosis.

Despite these promising results, several limitations warrant consideration. First, while murine models recapitulate key histopathological features of adenomyosis, interspecies differences in immune microenvironment and drug metabolism necessitate validation using primary human endometrial cells and patient-derived xenografts. Second, long-term safety beyond the 12-week observation period remains to be established, particularly regarding potential immune sensitization that may occur with repeated administration. Finally, comparative studies against clinical standards (*e.g.*, levonorgestrel-releasing intrauterine systems) are essential to establish the therapeutic superiority and cost-effectiveness of this approach.

In conclusion, this study demonstrates that MM-coated nanoparticles represent a promising therapeutic platform for managing adenomyosis, effectively combining targeted drug delivery with intrinsic anti-inflammatory properties. By bridging the gap between nanomedicine and innate immunology, this approach not only enhances treatment specificity and biocompat-

ibility but also offers a generalizable framework for addressing other inflammation-mediated gynecological conditions. The findings underscore both the theoretical significance of biomimetic nanomedicine and its practical potential for improving outcomes in conditions traditionally resistant to pharmacological intervention. Future efforts should prioritize clinical translation, including the development of scalable methods and compliance with regulatory standards in nanomanufacturing to enable broader therapeutic application of this technology.

Declaration of competing interest

The authors declare that they have no known competing financial interests or personal relationships that could have appeared to influence the work reported in this paper.

CRediT authorship contribution statement

Renwen Zhang: Writing – original draft, Visualization, Software, Conceptualization. **Yixing Zou:** Resources, Methodology. **Aihua Liao:** Writing – review & editing, Resources, Conceptualization. **Jing Luo:** Writing – original draft, Visualization, Methodology, Data curation, Conceptualization.

Acknowledgments

The authors gratefully acknowledged to Cheng Gao (University of Macau) for preparation of DG-NPs. Financial support was provided by the National Natural Science Foundation of China (No. 32270980 to J. Luo and No. 82220108008 to A. Liao).

Supplementary materials

Supplementary material associated with this article can be found, in the online version, at doi:10.1016/j.cclet.2025.111758.

References

[1] O. Yeniel, T. Cirpan, M. Ulukus, et al., Clin. Exp. Obstet. Gynecol. 34 (2007) 163–167.
[2] J.A. Abbott, Best Pract. Res. Clin. Obstet. Gynaecol. 40 (2017) 68–81.
[3] J. Naftalin, W. Hoo, K. Pateman, et al., Hum. Reprod. 27 (2012) 3432–3439.
[4] K.A. Kho, J.S. Chen, L.M. Halvorson, JAMA 326 (2021) 177–178.
[5] T. Capezzuoli, F. Toscano, M. Ceccaroni, et al., Best Pract. Res. Clin. Obstet. Gynaecol. 95 (2024) 102507.
[6] K.W. Schweppe, Maturitas 65 (2009) S23–S27.
[7] A. Etrusco, F. Barra, V. Chiantera, et al., Drugs 83 (2023) 1595–1611.
[8] S.W. Guo, Fertil. Steril. 119 (2023) 711–726.
[9] J.L. Eaton, Fertil. Steril. 116 (2021) 1578–1579.
[10] J. García-Solares, J. Donnez, O. Donnez, M.M. Dolmans, Fertil. Steril. 109 (2018) 371–379.
[11] J. Zhai, S. Vannuccini, F. Petraglia, L.C. Giudice, Semin. Reprod. Med. 38 (2020) 129–143.
[12] A. Ferenczy, Hum. Reprod. Updat. 4 (1998) 312–322.
[13] S.E. Bulun, S. Yildiz, M. Adli, J.J. Wei, Hum. Reprod. Updat. 27 (2021) 1086–1097.
[14] G. Leyendecker, L. Wildt, G. Mall, Arch. Gynecol. Obstet. 280 (2009) 529–538.
[15] M. Bourdon, P. Santulli, M. Jeljeli, et al., Hum. Reprod. Updat. 27 (2021) 108–129.
[16] H. Ota, S. Igarashi, J. Hatazawa, T. Tanaka, Hum. Reprod. Updat. 4 (1998) 360–367.
[17] J. Shi, Q. Xu, S. Yu, T. Zhang, Semin. Immunopathol. 47 (2025) 16.
[18] W. Niu, Y. Zhang, H. Liu, et al., J. Inflamm. Res. 16 (2023) 1949–1965.
[19] M. An, D. Li, M. Yuan, et al., Biol. Reprod. 96 (2017) 46–57.
[20] A. Shapouri-Moghaddam, S. Mohammadian, H. Vazini, et al., J. Cell. Physiol. 233 (2018) 6425–6440.
[21] K.P. Tremellen, P. Russell, J. Reprod. Immunol. 93 (2012) 58–63.
[22] Z. Xu, H. Zhou, T. Li, et al., Drug Resist. Updat. 75 (2024) 101098.
[23] J. Xin, X. Lu, J. Cao, et al., Adv. Mater. 30 (2024) e2404645.
[24] E.L. Etter, K.C. Mei, J. Nguyen, Adv. Drug Deliv. Rev. 179 (2021) 113994.
[25] K. Ying, Y. Zhu, J. Wan, et al., Bioact. Mater. 20 (2022) 449–462.
[26] X. Li, X. Ou, Z. Yang, et al., Adv. Mater. 37 (2025) e2416590.
[27] Y. An, C. Ji, H. Zhang, et al., ACS Nano 19 (2025) 11517–11546.
[28] S. Guo, Z. Li, L. Yan, Y. Sun, Y. Feng, Drug Des. Dev. Ther. 12 (2018) 1621–1631.
[29] B. Zhu, Y. Chen, X. Shen, X. Liu, S.W. Guo, Reprod. Biol. Endocrinol. 14 (2016) 66.
[30] X. Zhang, H. Yuan, L. Deng, et al., Hum. Reprod. 23 (2008) 2024–2030.
[31] Y. Shi, L. Xu, X. Wang, et al., Phytomedicine 127 (2024) 155461.
[32] Y. Liu, X. Wang, L. Wan, et al., Hum. Reprod. 35 (2020) 1377–1390.
[33] D. Chen, H. Qiao, Y. Wang, et al., Gene. Dis 7 (2020) 636–648.
[34] Y. Zhu, R. Shi, W. Lu, et al., Chin. Chem. Lett. 36 (2025) 110140.
[35] T. Zhang, C. Sun, S. Yang, et al., Chin. Chem. Lett. 35 (2024) 109248.
[36] Y. Li, Q. Jia, N. Liu, et al., Exploration (2025), doi:10.1002/exp.20240090.
[37] S. Zhang, M. Zhang, X. Li, et al., Molecules 27 (2022) 5973.
[38] Y. Deng, X. Zhang, H. Shen, et al., Front. Bioeng. Biotechnol. 7 (2019) 489.
[39] M. Wang, J. Zhao, H. Jiang, X. Wang, Mater. Horiz. 9 (2022) 1111–1140.
[40] G. Benagiano, I. Brosens, M. Habiba, Hum. Reprod. Updat. 20 (2014) 386–402.
[41] T. Feng, S. Wei, Y. Wang, et al., Biomed. Pharmacother. 94 (2017) 231–237.
[42] C. Gao, Q. Huang, C. Liu, et al., Nat. Commun. 11 (2020) 2622.
[43] R. Zhou, S. Xue, Y. Cheng, et al., J. Nanobiotechnol. 22 (2024) 578.
[44] W. Zhang, M. Wang, W. Tang, et al., Adv. Mater. 30 (2018) e1805557.
[45] Y. Ma, W. Gao, Y. Zhang, et al., ACS Appl. Mater. Interfaces 14 (2022) 6358–6369.
[46] H. Qu, J. Wu, Y. Pan, et al., ACS Nano 18 (2024) 28228–28245.
[47] H. Tang, W. Chu, J. Xiong, et al., Small 20 (2024) e2311967.
[48] Z. Yu, M. Wang, J. Li, et al., Small 21 (2025) e2410710.
[49] M. Yang, J. Zhou, L. Lu, et al., Exploration 4 (2024) 20230171.
[50] Y. He, S. Zhang, Y. She, et al., Exploration 4 (2024) 20230164.
[51] J. Liu, J. Chen, X. Zhang, et al., Chin. Chem. Lett. 35 (2024) 109779.
[52] Y. Gao, R. Zhou, Q. Wang, et al., Chin. Chem. Lett. 35 (2024) 109521.